

Development and Performance Assessment of a Novel Plasma p-Tau181 Assay Reflecting Tau Tangle Pathology in Alzheimer's Disease

AUTHORS/AFFILIATIONS:

Kenji Tagai^{1,2,7}, Harutsugu Tatebe^{1,7}, Sayo Matsuura¹, Zhang Hong¹, Naomi Kokubo¹,
Kiwamu Matsuoka¹, Hironobu Endo¹, Asaka Oyama¹, Kosei Hirata¹, Hitoshi Shinotoh¹,
Yuko Kataoka¹, Hideki Matsumoto^{1,3}, Masaki Oya¹, Shin Kurose^{1,4}, Keisuke Takahata^{1,4},
Masanori Ichihashi¹, Manabu Kubota¹, Chie Seki¹, Hitoshi Shimada^{1,5}, Yuhei Takado¹,
Kazunori Kawamura¹, Ming-Rong Zhang¹, Yoshiyuki Soeda⁶, Akihiko Takashima⁵,
Makoto Higuchi¹, Takahiko Tokuda^{1*}

¹ Institute for Quantum Medical Science, Quantum Life and Medical Science
Directorate, National Institutes for Quantum Science and Technology, Chiba 263-8555,
Japan

² Department of Psychiatry, The Jikei University of Medicine, Tokyo 105-8461, Japan

³ Department of Oral and Maxillofacial Radiology, Tokyo Dental College, Tokyo
101-0061, Japan

⁴ Department of Psychiatry, Keio University School of Medicine, Tokyo 160-0016,
Japan

⁵ Department of Functional Neurology & Neurosurgery, Center for Integrated Human
Brain Science, Brain Research Institute, Niigata University, Niigata 951-8585, Japan

⁶ Laboratory for Alzheimer's Disease, Department of Life Science, Faculty of Science,
Gakushuin University, Tokyo 171-8588, Japan

⁷ These authors contributed equally

* Correspondence: tokuda.takahiko@qst.go.jp

1 **Abstract:** Several blood-based assays for phosphorylated tau (p-tau) have been
2 developed to detect brain tau pathologies in Alzheimer's disease (AD). However, plasma
3 p-tau measured by currently available assays is influenced by brain amyloid and,
4 therefore, could not accurately reflect brain tau deposits. Here, we devised a novel
5 immunoassay that can quantify N- and C-terminally truncated p-tau fragments
6 (mid-p-tau181) in human plasma. We measured plasma p-tau181 levels in 164
7 participants who underwent both amyloid and tau positron emission tomography (PET)
8 scans using mid-p-tau181 and conventional p-tau181 assays. The mid-p-tau181 assay
9 displayed stronger correlations with tau PET accumulation than the conventional assay
10 in the AD continuum and accurately distinguished between tau PET-positive and
11 -negative cases. Furthermore, the mid-p-tau181 assay demonstrated a trajectory similar
12 to tau PET alongside cognitive decline. Consequently, our mid-p-tau181 assay could be
13 useful in evaluating the extent of brain tau burden in AD.

14
15 **Keywords:** Plasma biomarker, Tau phosphorylated at threonine 181 (p-tau181), Simoa,
16 Tau PET, Alzheimer's disease

17
18
19
20
21
22
23
24
25
26
27
28
29
30
31
32
33
34
35
36

1 Introduction

2 Estimates project that the number of people with dementia worldwide will reach
3 153 million by 2050¹, highlighting the urgent need to address the remarkable health and
4 social impacts of this condition. Alzheimer's disease (AD), the most prevalent form of
5 dementia, has been characterized as the deposit of two abnormal proteins, namely
6 amyloid- β (A β) and tau, in the brain. Over the years, numerous disease-modifying
7 therapies (DMTs) targeting these abnormal proteins have been developed², with the
8 Food and Drug Administration (FDA) having recently approved several DMTs targeting
9 A β due to their efficacy in decreasing brain amyloid deposition and modestly slowing
10 AD progression³⁻⁵. Researchers anticipate that these DMTs will be increasingly utilized
11 in clinical practice, with the potential for developing additional DMTs targeting not only
12 A β but also tau in the near future⁶.

13 Biomarkers have become an integral part of clinical trials on DMTs given their
14 widespread use for subject recruitment and outcome measurements². The
15 amyloid/tau/neurodegeneration (A/T/N) biomarker classification system had been
16 proposed for the biological staging of AD⁷. In particular, positron emission tomography
17 (PET) has emerged as a well-established imaging biomarker for assessing the
18 accumulation of A β and tau in the brain⁸, playing a critical role in evaluating novel
19 DMTs^{4,9}. The noteworthy decline in amyloid accumulation based on PET findings¹⁰
20 may have expedited the FDA approval of aducanumab². Moreover, incorporating tau
21 PET as a screening measure, assuming that high tau accumulation may cause resistance
22 to anti-amyloid therapy, may have played a part in the success of the donanemab
23 clinical trial^{4,11}. Despite their usefulness, PET scans are not ideal for frequent
24 assessment or large-scale screening given their limited availability, high cost, and
25 radiation exposure¹². Similarly, A β and p-tau in the cerebrospinal fluid (CSF) have also
26 been accepted as standard biomarkers for qualifying AD pathology^{13,14}. However, CSF
27 testing has seen somewhat limited use considering its invasiveness, low-throughput
28 nature, and need for expertise during CSF sampling^{12,15}. Based on the present
29 circumstances surrounding the development of biomarkers for AD, one of the most
30 critical unmet needs has been the identification of blood-based biomarkers closely
31 correlated with tau PET parameters that reflect brain tau burden, especially in the
32 context of selecting suitable patients for anti-amyloid therapies.

33 Recent advances in measurement methodologies have made it possible to quantify
34 minute amounts of proteins in the peripheral blood that are associated with brain
35 diseases, thereby enabling the feasibility of blood-based biomarkers¹⁵. Notably, there is
36 growing evidence for the clinical significance of plasma phosphorylated tau (p-tau)

assays in detecting AD pathology^{16–19}, similar to CSF biomarkers. The C-terminal portion of the tau protein, which predominantly constitutes neurofibrillary tangles²⁰, is seldom detectable in biofluids^{21–23}. Most of the current immunoassays for plasma p-tau, therefore, employ a pair of antibodies, one of which recognizes the phosphorylated residues, such as Thr181, Thr217, and Thr231, in the mid-portion, while the other identifies the N-terminal region of the tau protein. Accordingly, currently available immunoassays for plasma p-tau detect C-terminally truncated p-tau containing the N-terminus to the mid-domain (N-p-tau)¹². Plasma p-tau levels quantified using these N-p-tau assays can accurately differentiate between AD pathology and other tauopathies with high diagnostic accuracy^{17,18,24,25} and help predict future cognitive decline from prodromal phases^{26,27}. However, one of the significant problems in the clinical use of N-p-tau assays is their inability to be considered as a surrogate marker for tau burden in the brain²⁸ given that the measurements obtained had a more pronounced association with amyloid PET than with tau PET^{29–32}. Therefore, the need for developing blood-based tau biomarkers strongly correlated with PET-detectable tau accumulations in the brain remains unmet.

The present study aimed to formulate a novel p-tau assay that can be interchangeable with the tau PET study. Considering that the truncation of the N-terminal of the tau protein may occur subsequent to the truncation of its C-terminal with the formation of neurofibrillary tangle³³, we hypothesized that the levels of both N- and C-terminally truncated p-tau181 fragments could be correlated with the abundance of tau aggregates in the brain. Thus, we developed a novel mid-region-directed p-tau181 assay by modifying the formerly established N-p-tau181 assay¹⁶. To validate our hypothesis, we collected plasma samples from subjects who underwent PET with both ¹¹C-Pittsburgh Compound B (¹¹C-PiB) and ¹⁸F-florozotau (aka PM-PBB3/APN-1607) for the examination of Aβ and tau depositions in the brain, respectively.^{34,35} We demonstrated a strong correlation of between plasma levels of p-tau181 fragments measured using our mid-region-directed assay (hereinafter called mid-p-tau181) and tau PET tracer retention but no linear correlation between plasma N-p-tau181 levels and tau PET data, suggesting the clinical usefulness of the novel assay as a surrogate biomarker for PET-visible tau pathologies.

32

33 Results

34 *Validation of the newly developed mid-p-tau181 assay*

35 The plasma mid-p-tau181 assay exhibited high analytical performance (Supplementary
36 Methods and Results, Supplementary Tables 1–3, Supplementary Figures 1–5), with high

precision within and between runs. Spike recovery experiments and parallelism of serially diluted plasma samples confirmed the reliability of the measurements.

Demographic data

Table 1 summarizes the demographic information of the participants. All participants (n = 164) underwent neuropsychological assessment, including the Clinical Dementia Rating (CDR) scale, Mini-Mental State Examination (MMSE), and frontal assessment battery (FAB), simultaneous amyloid and tau PET imaging, and blood sampling on the day of the PET examination. Cognitively normal (CN) individuals exhibiting negative results on amyloid and tau PET imaging were designated into the CN cohort. Patients with mild cognitive impairment (MCI) and AD who had positive amyloid PET findings were categorized into the AD continuum group (dubbed AD group). Furthermore, subjects with progressive supranuclear palsy (PSP) and other frontotemporal lobar degeneration (FTLD) who had negative amyloid PET findings were classified into the PSP and FTLD cohorts, respectively. No significant differences in age, years of schooling, and gender were observed among the groups. All patient groups showed lower MMSE (CN, 29.3 ± 1.0 ; AD, 21.9 ± 4.1 ; PSP, 24.8 ± 5.8 ; FTLD, 23.8 ± 6.1) and FAB scores (CN, 16.7 ± 1.2 ; AD, 13.0 ± 3.0 ; PSP, 12.0 ± 3.6 ; FTLD, 11.0 ± 4.8) than the CN group ($p < 0.05$, Table 1). Notably, 90% of the AD group comprised subjects with early-stage AD who had a CDR score of 0.5 or 1 accounted; however, the mean MMSE scores of this group were lower than those of the PSP group ($p < 0.05$, Table 1) but did not significantly differ from those of the FTLD group.

Significant linear correlation between plasma mid-p-tau181 but not N-p-tau181 with tau PET findings in patients with AD continuum

We found a significant linear correlation between the plasma mid-p-tau181 levels and tau PET tracer retention in patients with AD continuum (Figure 1). Voxel-wise analyses revealed a positive correlation between plasma mid-p-tau181 levels and tracer binding in the temporal and parietal cortices [Figure 1A; $p < 0.05$, corrected for family-wise error (FWE)]. This finding was corroborated by the following three different quantitative indices based on a region of interest (ROI): (1) standardized uptake value ratio (SUVr)³⁶ in the temporal meta-ROI that characterizes tau lesions in AD³⁷; (2) AD tau score, which is a machine learning-based measure indicating AD-related features of tau PET images³⁵; and (3) Braak staging SUVrs based on the neuropathological hypothesis³⁶ (Supplementary Figure 6). These AD signature ROI analyses revealed significant linear correlations between plasma mid-p-tau181 levels and temporal meta-ROI SUVrs ($r =$

0.506; $p = 0.0003$), AD tau scores ($r = 0.556$; $p = 0.0003$), and SUVRs in the Braak stage III/IV limbic ($r = 0.403$; $p = 0.003$) and V/VI neocortical ($r = 0.508$; $p = 0.0003$) but not Braak stage I/II entorhinal ($r = 0.216$; $p = 0.149$) ROIs. These findings clearly demonstrate that plasma mid-p-tau181 levels could accurately reflect AD-related tau accumulation that spreads from the entorhinal cortex first to the inferior temporal lobe and then to the parieto-occipital regions of the neocortex but not tau accumulation in the Braak I/II region.

Conversely, the conventional N-p-tau181 assay (Simoa pTau-181 Advantage V2.1 kit, Quanterix, MA, USA) showed no significant linear correlations with tau PET tracer retention (Figure 2). Voxel-based analysis revealed a weak correlation between the aforementioned parameters in the temporal cortex (Figure 2A; $p < 0.05$, uncorrected); however, no significant correlation was observed upon correction for multiple comparisons ($p < 0.05$, FWE-corrected). Moreover, none of the three ROI-based analyses revealed significant linear correlations between N-p-tau181 levels and PET parameters ($p < 0.05$, after Bonferroni's correction). Instead, these examinations showed inverse U-shaped nonlinear correlations between plasma N-p-tau181 levels and tau PET SUVRs in the temporal meta-ROI ($R^2 = 0.402$), AD tau score ($R^2 = 0.147$), and Braak stage III/IV ($R^2 = 0.307$) and V/VI ROIs ($R^2 = 0.223$) but not Braak stage I/II ROIs (Figure 2B, C).

Discriminating between tau PET statuses using plasma mid-p-tau181 levels

Using three different ROI-based methods, we qualitatively assessed the PET-detectable tau burden in the CN subjects and AD continuum patients. Thereafter, receiver operating characteristic (ROC) curve analyses were conducted to determine plasma mid-p-tau181 cutoff levels for discriminating between individuals with positive and negative AD-type tau PET findings. The PET finding classification was based on the cutoff values of imaging-based Braak staging, temporal meta-ROI SUVR, and AD tau score. The Braak stage in each subject was determined according to the ROI with the highest Z-score (see Methods for detailed procedures), with stages 0 and I/II indicating tau-negative and stages III/IV and V/VI being classified as tau-positive (Supplementary Table 4). The cutoff values for the meta-ROI SUVR and AD tau score were determined using ROC curve analyses in the current and previous studies³⁵, respectively. Consequently, our findings showed that tau-positive AD cases had significantly higher plasma mid-p-tau181 concentrations than did tau-negative AD and CN cases (Figure 3A; $p < 0.0001$). Furthermore, area under the ROC curve (AUC) values during ROC analyses of mid-p-tau181 levels to different between tau PET positivity and negativity defined by all three methods exceeded 0.85 (Table 2, Figure 3B), indicating that this plasma

biomarker with reference to PET-based classifications had robust discriminative power.

Head-to-head comparisons between two p-tau181 assays according to their correlation with non-tau imaging biomarkers

Next, we examined whether plasma p-tau181 levels determined by either the pre-established or newly developed assay were correlated with the abundance of cerebral amyloid accumulations evaluated using PiB-PET (Supplementary Figure 7). Notably, none of the measures obtained using these p-tau181 assays were correlated with voxel-based and ROI-based quantitative values of amyloid burden. Meanwhile, voxel-based morphometry revealed significant negative correlations between the plasma mid-p-tau181 concentration and gray matter volume in the neocortex, primarily in the temporal and parietal areas (Figure 4). The ROI-based analysis also confirmed a correlation between mid-p-tau181 and cortical thinning in AD-signature regions defined as described elsewhere³⁸ ($r = -0.406$; $p = 0.005$). In contrast, N-p-tau181 did not exhibit any correlation with structural imaging measures.

Comparison among blood-based biomarkers according to diagnostic performance for AD

Figure 5A illustrates group comparisons of four AD-related plasma biomarkers, including the mid-p-tau181 measured using our in-house assay, with-and the corresponding values for each diagnostic group being presented in Table 1. Our results indicated significant differences in A β 42/40 and N-p-tau181 concentrations between the AD and other groups. Additionally, the AD group exhibited significantly higher mid-p-tau181 concentrations than did all other groups except the PSP group. Moreover, all disease groups had increased neurofilament light chain (NfL) concentrations compared to the CN group. ROC curve analyses (Figure 5B) revealed the following order of biomarkers according to their ability to discriminate between individuals with and without ¹¹C-PiB-PET-positive amyloid pathology when all participants were incorporated: N-p-tau181 (AUC = 0.867), A β 42/40 (AUC = 0.850), mid-p-tau181 (AUC = 0.771), and NfL (AUC = 0.555).

Trajectory analyses of imaging- and blood-based A/T/N biomarkers along with cognitive decline in the CN and AD continuum subjects

The imaging biomarkers examined in this cohort revealed that the A marker (i.e., amyloid PET index) displayed a sigmoidal trajectory when plotted against cognitive deficits and reached a plateau when the MMSE score was around 20 points, the point at

which cognitive decline became apparent (Figure 6A). Conversely, the T marker (i.e., tau PET index) displayed a linearly progressive increase with a decrease in the MMSE scores. The N marker (i.e., the volumetric MRI index) also tended to show a linear increment similar to that for the T marker, albeit with a lesser z-score range.

The blood-based biomarkers displayed trajectories closely resembling those of the imaging biomarkers, although their dynamic ranges were inferior to those of the imaging biomarkers (Figure 6B). Notably, the two different blood-based T markers showed clearly distinct trajectories such that plasma mid-p-tau181 levels exhibited a linearly progressive increase similar to the tau PET index with the decline in MMSE scores, whereas plasma N-p-tau181 levels measured using a currently widely used conventional p-tau assay (Quanterix) displayed a sigmoidal trajectory similar to that for amyloid PET with the decrease in MMSE scores. The A (A β 42/40) and N (NfL) markers showed a sigmoidal curve and a linear progression, respectively, similar to those for the corresponding imaging biomarkers.

Discussion

The current study aimed to develop a novel plasma p-tau biomarker (mid-p-tau181) that could be potentially interchangeable with tau PET imaging and validate its ability to accurately reflect the extent of AD-type tau burden in the brain confirmed using tau PET. Notably, our results showed that the plasma mid-p-tau181 exhibited a strong correlation with the accumulation of tau PET ligands in AD brains and was accordingly able to discriminate positive and negative AD pathologies on tau PET. These findings indicate that plasma mid-p-tau levels could have sufficient accuracy in determining the existence of AD-type tau pathology in the brain without being affected by brain amyloid deposition, which has been known to affect the plasma levels of N-terminal to mid-domain forms of p-tau181 (N-p-tau) detected as plasma p-tau181 by most conventional p-tau assays.^{17,26} Moreover, the trajectory of the change in the plasma levels of the mid-p-tau181 along with MMSE scores was similar to that observed with tau PET. These results strongly suggest the potential utility of plasma mid-p-tau181 as a blood-based biomarker for the detection and stratification of AD-type tau burden in the brain, mainly in the tau accumulation phase of the AD continuum.

Various experimental and clinical studies have suggested that an increase in soluble p-tau in biofluids could be strongly associated with A β aggregation.^{17,29,30,39–42} This evidence indicates that tau hyperphosphorylation occurs in neurons exposed to A β , with p-tau levels increasing in response to A β deposition. Consistent with this notion, plasma p-tau is highly valuable for distinguishing AD from other neurodegenerative

1 diseases.^{18,43–45} In addition, p-tau concentrations measured using conventional N-p-tau
2 assays have been recognized as an early marker for AD given the increase in their
3 values alongside A β deposition^{17,44,46–49} rather than before tau aggregation.^{19,28,30}
4 Meanwhile, the process of tangle maturation also needs to be considered when
5 interpreting the levels of soluble p-tau in biofluids measured using immunoassay
6 methodologies. Most current approaches for quantifying soluble p-tau via immunoassay
7 predominantly target tau fragments phosphorylated at positions 181, 217, or 231 and
8 bearing N-terminal epitopes.¹² The C-terminal portion of the tau protein, which is
9 involved its aggregation,⁵⁰ is rarely present in soluble species of the tau protein. Thus,
10 soluble tau fragments present in the body fluids usually include only the
11 N-terminal-to-mid-region epitopes, ensuring consistent quantification using N-p-tau
12 assays currently accessible.¹² Conversely, N-terminal cleavage also occurs in addition to
13 its C-terminal cleavage in tau proteins insolubilized and deposited in the brain, which
14 has been postulated to play a role in tangle evolution.^{33,51–53} Therefore, this tau
15 truncation implies that the accumulation of tau aggregates in the brain might not directly
16 correspond with soluble p-tau quantified using conventional N-p-tau assays. Concurrent
17 with this perspective, a study investigating the associations between various plasma
18 p-tau species and amyloid/tau PET demonstrated that all plasma p-tau species measured
19 by N-p-tau assays showed a considerably stronger correlation with amyloid PET
20 binding than with tau PET binding.³⁰ These findings support the notion that currently
21 available p-tau assays cannot be interchangeable with tau PET given that they do not
22 accurately coincide with tau PET results and are also affected by amyloid deposition.
23 Conversely, our mid-p-tau181 assay demonstrated a strong correlation with tau
24 PET accumulation, but not with the amyloid PET ligand, in AD brains. The tau PET
25 ligand employed in the current study, namely Florzortau, exhibits high sensitivity to
26 AD-specific tau lesions, including neurofibrillary tangles, neuropil threads, and neuritic
27 plaques.³⁴ This suggests that our plasma mid-p-tau181, which is a previously
28 nonexistent blood-based “T” biomarker in the ATN framework, corresponded to the
29 AD-type tau accumulation in tau PET scans.
30 Moreover, the characteristics of mid-p-tau181 suggest its usefulness as a biomarker
31 for predicting the therapeutic response to current DMTs targeting A β . These therapies
32 are more likely to be effective when introduced before substantial tau aggregation.
33^{2,11,54,55} Therefore, identifying patients with high plasma mid-p-tau levels, in whom
34 brain tau aggregation has been suggested to have progressed beyond the critical point,
35 could help select patients more likely to benefit from DMTs targeting A β , like so in the
36 phase 3 study of donanemab.¹¹ Our results showed that our plasma mid-p-tau181 could

discriminate between tau-positive and -negative subjects with a specificity greater than 85%, effectively excluding patients with advanced tau pathology.

Plasma mid-p-tau181 levels were also correlated with brain atrophy and increased with the progression of cognitive impairment evaluated using MMSE scores during trajectory analysis. Meanwhile, plasma N-p-tau181 levels increased in the early stage even when MMSE scores were within the normal range, and its increase slowed down in the later phase when cognitive impairment advanced. In support of these findings, CSF p-tau181 measured with an immunoassay targeting the mid-portion of tau protein also increased later than N-p-tau181,⁴⁹ as observed in our study. However, the increase in CSF N-p-tau181 species ceased and instead decreased after neuronal dysfunction started in the familial AD cohort.⁵⁶ Consequently, plasma mid-p-tau181 has been associated with the later stages of AD in contrast to N-p-tau181, which has been associated with the early stage just after amyloid deposition starts. Mid-p-tau181 could thus be utilized as a biomarker to monitor disease progression when cognitive impairment starts worsening due to tau accumulation in the brain.

The PSP group also showed a significant elevation in plasma mid-p-tau181, deviating from the results of the N-p-tau assay and leading to a slight decrease in specificity to AD. Phosphorylation in the mid-region has also been observed in non-AD tauopathies, such as PSP,⁵⁷ with some previous studies reporting that soluble p-tau levels in CSF might be elevated in non-AD tauopathies.^{58,59} However, plasma mid-p-tau181 levels were not correlated with tau PET accumulation in the PSP patients (Supplementary Figure 8). Accordingly, the underlying pathophysiological basis for the observed increase in plasma mid-p-tau181 levels in our PSP group remains elusive. Although further investigations are still needed, plasma mid-p-tau181 might be a valuable biomarker for non-AD tauopathies.

This study has several limitations worth noting. Firstly, our sample size was modest, and longitudinal data was absent. As such, we are planning to conduct more studies in the near future to address these limitations. Secondly, we found that no correlation between the extent of amyloid burden in the brain evaluated through amyloid PET and not only plasma mid-p-tau181 levels but also N-p-tau181 levels in contrast to previous reports, which have shown a positive correlation between brain amyloid burden and plasma N-p-tau.^{26,30,32} This discrepancy may be attributed to the demographics of the patients with AD continuum included in the current study, who predominantly comprise symptomatic AD cases and whose amyloid deposition in the brain has already plateaued. To confirm this phenomenon, we conducted correlation analyses between plasma p-tau181 levels and PET findings in the study participants,

1 including both the CN and AD continuum subjects (Supplementary Figure 9).
2 Consistent with previous reports,^{30,32} plasma N-p-tau181 levels were primarily
3 correlated with amyloid PET results, whereas plasma mid-p-tau181 levels were
4 correlated chiefly with tau PET results. Further validation of interactions between
5 plasma p-tau species and amyloid/tau PET results are still required in independent
6 cohorts, including very early AD cases, such as those with asymptomatic AD [A(+)/T(-)].
7 Additional validation studies using alternative tau PET tracers, such as ¹⁸F-MK6240,
8 would certainly be informative. Moreover, although this study developed the
9 mid-p-tau181 assay, the characteristics of plasma p-tau biomarkers, including which AD
10 continuum stages a specific plasma p-tau molecule could reflect most, could vary
11 depending on the phosphorylation site on the p-tau molecules.^{56,60} Given some previous
12 reports indicating a moderate correlation between p-tau217 and tau pathologies in the
13 AD brain,^{18,19,32} it is also intriguing to develop other assays targeting mid-p-tau species
14 with phosphorylation sites other than 181.

15 Despite these limitations, the strength of the present study lies our development of
16 an innovative mid-p-tau assay that corresponds with the AD-type brain tau burden
17 determined using tau PET and its validation in a cohort of controls and AD continuum
18 subjects who underwent both amyloid- and tau PET. Although specific assays have been
19 reported to measure tau fragments in the CSF and exhibit correlations with brain tau
20 pathologies,^{61,62} there are still unmet needs for implementing comprehensively validated
21 blood-based biomarkers that accurately reflect brain tau burden without being
22 influenced by amyloid deposition. Our novel mid-p-tau assay is anticipated to function
23 as a blood-based biomarker for the screening and monitoring of brain tau pathologies,
24 especially in the selection of patients most suitable for anti-A β DMTs and the
25 development of tau-targeted therapies, although further longitudinal studies and
26 validation in larger cohorts are necessary.

27 **Methods**

28 ***Participants***

29 We recruited a cohort of 186 individuals comprising 43 CN individuals, 30 patients with
30 MCI due to AD, 31 patients with dementia due to AD, 52 patients with PSP, and 30
31 patients with other FTLN syndromes between January 2018 and September 2022. The
32 other FTLNs comprised 12 cases with corticobasal syndrome (CBS), 10 cases with
33 behavioral-variant frontotemporal dementia (BvFTD), 7 cases with frontotemporal
34 dementia and parkinsonism linked to chromosome 17 MAPT (FTDP-17/MAPT), and 1
35 case of primary progressive aphasia. CN individuals were those aged older than 40 years
36

who had no history of neurological and psychiatric disorders, had a MMSE score of ≥ 28 , or had a Montreal Cognitive Assessment score of ≥ 26 and Geriatric Depression Scale score of ≤ 5 .³⁵ Patients with MCI and dementia due to AD underwent clinical evaluations. Cognitive impairment severity was defined as MMSE < 24 and CDR ≥ 1 for dementia and MMSE ≥ 26 and CDR = 0.5 for MCI.³⁵ Patients with PSP and other FTLT syndromes were diagnosed according to established criteria previously reported.^{34,35}

In the present study, the diagnosis of patients with MCI and dementia due to AD required brain amyloid positivity in PET scans, and they were combined and categorized into the AD group based on the concept of the AD continuum. We excluded patients with PSP and other FTLT who had positive amyloid PET results to eliminate the influence of mixed pathology. Those with other FTLTs were heterogeneous and categorized into the FTLT group. Furthermore, CN individuals with a positive result on either or both amyloid and tau PET scans were also excluded as they were considered to have been in the preclinical AD stage. Amyloid positivity was defined based on ¹¹C-PiB-PET visual inspection performed by a minimum of three specialists with expertise in the field.³⁴ Tau PET negativity in CN individuals was defined according to the AD tau score (< 0.1986) and PSP tau score (< 0.3431) as reported previously.³⁵ These scores, which were calculated from ¹⁸F-florotau PET images via our established machine learning algorithm, possess a high degree of sensitivity and specificity in discriminating CN individuals from patients with AD and PSP.³⁵ Consequently, after excluding 3 CN individuals and 11 MCI, 2 AD, 2 PSP, and 4 FTLT patients according to the aforementioned criteria, our final cohort consisted of 164 participants comprising 40 CN individuals and 48 AD, 50 PSP, and 26 FTLT patients.

This study was approved by the National Institutes for Quantum Science and Technology Certified Review Board. Written informed consent was obtained from all participants and spouses or close family members when participants were cognitively impaired. This study was registered with the UMIN Clinical Trial Registry (UMIN-CRT; number 000041383).

Blood sampling

We obtained blood samples through venous puncture on the same day as the PET scan. A total of 8 mL of blood was collected in ethylenediaminetetraacetic acid (EDTA)-containing tubes. After collection, plasma was separated by centrifugation for 10 min at 2000g, aliquoted into polypropylene tubes, and then stored at -80°C until analysis.

Measurements of blood biomarkers

1 We developed a novel immunoassay able to quantify plasma levels of both N- and
2 C-terminally truncated p-tau181 fragments run on a highly sensitive automated digital
3 ELISA platform (Simoa HD-X Analyzer, Quanterix, Lexington, KY, USA) and measured
4 the levels of p-tau181 including such fragments in human plasma. The details of the
5 procedures for method validation of this original immunoassay are described in the
6 Supplementary Methods and Results. We also quantified plasma levels of the A/T/N
7 biomarkers⁷ (A β 42, A β 40, p-tau181, and NfL instead of total tau in the original paper)
8 utilizing the Simoa platform (Quanterix) equipped with validated assay kits. Procedures
9 were performed following the manufacturer's instructions. This study employed the
10 A β 42/A β 40 ratio as a proxy for cerebral amyloid burden. Plasma p-tau181 measured
11 using the commercial kit (Simoa pTau-181 V2.1 Assay, Quanterix) was defined as
12 N-p-tau181, whereas plasma p-tau181 measured using the originally developed
13 immunoassay run on the Simoa system was defined as mid-p-tau181.

14 All plasma samples were diluted four times with the respective sample diluent
15 before the assays to minimize matrix effects. All plasma samples were run in duplicate
16 with the same lot of standards. The relative concentration estimates of plasma biomarkers
17 were calculated according to their respective standard curves.

18

19 ***PET and MRI data acquisition***

20 Amyloid and tau deposits in the brains of all participants were assessed using PET with
21 ¹¹C-PiB and ¹⁸F-florzorotau as described in other clinical trials (UMIN-CRT; number
22 000026385, 000026490, 000029608, 000030248, and 000043458). One PSP patient who
23 had already been confirmed to be A β -negative at another facility no longer underwent
24 ¹¹C-PiB-PET at our center. The scan protocol was described as follows: parametric
25 ¹¹C-PiB-PET images were acquired 50–70 min after injection (injected dose: 528.5 ± 65.5
26 MBq, molar activity 90.2 ± 26.2 GBq/ μ mol); ¹⁸F-florzorotau PET images were obtained
27 90–110 min after injection (injected dose: 186.6 ± 7.4 MBq, molar activity 244.2 ± 86.7
28 GBq/ μ mol). PET was primarily conducted using a Biograph mCT flow system (Siemens
29 Healthcare), with some cases using the Discovery MI (GE Healthcare) (9 ¹¹C-PiB scans
30 in CN individuals; 22 ¹¹C-PiB scans and 3 ¹⁸F-florzorotau scans in AD patients; 7 ¹¹C-PiB
31 scans in PSP patients; and 4 ¹¹C-PiB scans in FTLN patients) and an ECAT EXACT HR+
32 scanner (CTI PET Systems, Inc.) (three ¹¹C-PiB scans in CN individuals, four ¹¹C-PiB
33 scans in AD patients, nine ¹¹C-PiB scans in PSP patients, and three ¹¹C-PiB scans in
34 FTLN patients). Acquired PET images were reconstructed using the filtered back
35 projection method with a Hanning filter. MRI examination was conducted simultaneously
36 with PET using a 3-T scanner (MAGNETOM Verio; Siemens Healthcare). The

anatomical images were acquired using a three-dimensional T1-weighted gradient echo sequence that produced a gapless series of thin sagittal sections (TE = 1.95 ms, TR = 2300 ms, TI = 900 ms, flip angle = 9°, acquisition matrix = 512 × 512 × 176, voxel size = 1 × 0.488 × 0.488 mm³).

Imaging analyses

All images were preprocessed using PMOD software (version 4.3, PMOD Technologies Ltd), FreeSurfer 6.0 (<http://surfer.nmr.mgh.harvard.edu/>), MATLAB (The Mathworks, Natick, MA, USA), and Statistical Parametric Mapping software (SPM12, Wellcome Department of Cognitive Neurology). PET images were co-registered with individual anatomical T1-weighted MR images, and SUVR images were generated using each reference region. The cerebellar cortex was the reference region for the ¹¹C-PiB-PET images. For ¹⁸F-florbetapir PET images, an optimized reference region was set through an in-house MATLAB script that considered the distribution of diverse tau lesions throughout the entire gray matter and extracted optimized reference regions on an individual basis.⁶³ Each PET and MR image was also normalized to the Montreal Neurologic Institute space using the Diffeomorphic Anatomical Registration Through Exponentiated Lie Algebra (DARTEL) algorithm and was smoothed with a Gaussian kernel at 8-mm full-width at half maximum in voxel-wise analyses.

We performed an ROI analysis targeting AD pathologies on each imaging modality to quantify the regional amyloid/tau burden and cortical thinning. The amyloid burden was assessed using a Centiloid atlas (frontal, temporal, parietal, precuneus, anterior striatum, and insula) implemented in the PMOD Neuro Tool (PMOD Technologies Ltd). Each Centiloid SUVR was calculated and converted to a Centiloid score (CL score)⁶⁴ using PET data from 12 young CN individuals aged 23–43 years and 25 cases of AD patients scanned at our institution. Tau burden was assessed using ROIs targeting tau pathology associated with AD labeling through FreeSurfer, Braak staging ROIs (I/II, III/IV, V/VI),³⁶ and temporal meta-ROI (entorhinal, amygdala, parahippocampal, fusiform, inferior temporal, and middle temporal).³⁷ We excluded the hippocampus from the Braak stage I/II ROI because of potential spill-in from the choroid plexus.³⁴ Additionally, we also estimated the AD tau score to assess AD-type tau burden in the brain, which was calculated using an Elastic Net model trained on tau PET data as previously reported.³⁵ A qualitative analysis based on the values obtained from these ROI analyses was also conducted to evaluate the presence of tau lesions. For Braak staging, the SUVR values were converted to z-values based on another young CN cohort, and the highest stage was assigned based on the average regional Z-score (>2.5).

Those with stages 0–I/II were classified as tau-negative, whereas those with stages III/IV–V/VI were classified as tau-positive. The cutoff value of temporal meta-ROI SUVR was set at 1.105 to maximize the differentiation between CN individuals and AD patients during ROC analysis (see Supplementary material for detailed information). and the cutoff value of AD tau score was set at 0.1986 as described elsewhere.³⁵ Cortical thickness was measured using the cortical signature of AD through FreeSurfer (medial temporal, inferior temporal, temporal pole, angular, superior frontal, superior parietal, supramarginal, precuneus, and middle frontal).³⁸

Statistical analyses

Statistical analyses were conducted using GraphPad Prism version 9 (GraphPad Software). Initially, group comparisons were performed using the Kruskal–Wallis test or Mann–Whitney U test for demographic data and measured blood biomarker values and Fisher's exact test for gender ($p < 0.05$, corrected by Dunn's multiple comparisons). Subsequently, correlation analyses were conducted to verify the association between each p-tau181 assay and each imaging biomarker. During voxel-based analyses, a linear regression model was applied using SPM12. The extent threshold was established based on the expected voxels per cluster. For multiple voxel comparisons, family-wise error corrections at the cluster level were applied ($p < 0.05$, FWE-corrected). During ROI-based analyses, Pearson's correlation analyses were performed ($p < 0.05$, corrected by Bonferroni multiple comparisons), and nonlinear regression analysis (quadratic) was conducted when no significant correlation was observed. Results were adopted when the nonlinear analysis based on Akaike's Information Criterion (AIC) showed a better fit than the linear one. In addition, ability of each blood biomarker to discriminate between the presence or absence of AD pathology, as defined by amyloid or tau PET positivity, was also evaluated by calculating AUC values from ROC curve analyses. The Youden index maximizing sensitivity plus specificity minus one determined the optimized cutoff value. Finally, to explore the trajectories from CN to AD for each blood/imaging biomarker, we converted each biomarker value to a z-value based on CN data. Thereafter, we examined their relationship with cognitive dysfunction (MMSE score). A linear or sigmoidal 4PL regression analysis was adapted, and the better-fitting model was selected based on AIC.

Data availability

The data supporting this study's findings are available from the corresponding author on reasonable request. Sharing and reuse of data require the expressed written permission of the authors, as well as clearance from the Institutional Review Boards.

References

1. Nichols, E. *et al.* Estimation of the global prevalence of dementia in 2019 and forecasted prevalence in 2050: an analysis for the Global Burden of Disease Study 2019. *The Lancet Public Health* **7**, e105–e125 (2022).
2. Cummings, J. *et al.* Alzheimer’s disease drug development pipeline: 2022. *Alzheimers Dement. (N. Y.)* **8**, e12295 (2022).
3. EMERGE and EMERGE and ENGAGE Topline Results: Two Phase 3 Studies to Evaluate Aducanumab in Patients With Early Alzheimer’s Disease (<https://investors.biogen.com/static-files/ddd45672-9c7e-4c99-8a06-3b557697c06f>). 2019.
4. Sims, J. R. *et al.* Donanemab in early symptomatic Alzheimer disease: The TRAILBLAZER-ALZ 2 randomized clinical trial. *JAMA* **330**, 512–527 (2023).
5. van Dyck, C. H. *et al.* Lecanemab in early Alzheimer’s disease. *N. Engl. J. Med.* **388**, 9–21 (2023).
6. Imbimbo, B. P., Ippati, S., Watling, M. & Balducci, C. A critical appraisal of tau-targeting therapies for primary and secondary tauopathies. *Alzheimers. Dement.* **18**, 1008–1037 (2022).
7. Jack, C. R., Jr *et al.* NIA-AA Research Framework: Toward a biological definition of Alzheimer’s disease. *Alzheimers. Dement.* **14**, 535–562 (2018).
8. Villemagne, V. L., Doré, V., Burnham, S. C., Masters, C. L. & Rowe, C. C. Imaging tau and amyloid- β proteinopathies in Alzheimer disease and other conditions. *Nat. Rev. Neurol.* **14**, 225–236 (2018).
9. Teng, E. *et al.* Safety and efficacy of semorinemab in individuals with prodromal to mild Alzheimer disease: A randomized clinical trial. *JAMA Neurol.* **79**, 758–767 (2022).
10. Sevigny, J. *et al.* The antibody aducanumab reduces A β plaques in Alzheimer’s disease. *Nature* **537**, 50–56 (2016).
11. Mintun, M. A., Wessels, A. M. & Sims, J. R. Donanemab in early Alzheimer’s disease. Reply. *The New England journal of medicine* vol. 385 667 (2021).
12. Karikari, T. K. *et al.* Blood phospho-tau in Alzheimer disease: analysis, interpretation, and clinical utility. *Nat. Rev. Neurol.* **18**, 400–418 (2022).
13. Dubois, B. *et al.* Advancing research diagnostic criteria for Alzheimer’s disease: the IWG-2 criteria. *Lancet Neurol.* **13**, 614–629 (2014).
14. McKhann, G. M. *et al.* The diagnosis of dementia due to Alzheimer’s disease: recommendations from the National Institute on Aging-Alzheimer’s Association

- 1 workgroups on diagnostic guidelines for Alzheimer's disease. *Alzheimers. Dement.*
- 2 **7**, 263–269 (2011).
- 3 15. Hansson, O. *et al.* The Alzheimer's association appropriate use recommendations
- 4 for blood biomarkers in Alzheimer's disease. *Alzheimers. Dement.* **18**, (2022).
- 5 16. Tatebe, H. *et al.* Quantification of plasma phosphorylated tau to use as a biomarker
- 6 for brain Alzheimer pathology: pilot case-control studies including patients with
- 7 Alzheimer's disease and down syndrome. *Mol. Neurodegener.* **12**, 63 (2017).
- 8 17. Karikari, T. K. *et al.* Blood phosphorylated tau 181 as a biomarker for Alzheimer's
- 9 disease: a diagnostic performance and prediction modelling study using data from
- 10 four prospective cohorts. *Lancet Neurol.* **19**, 422–433 (2020).
- 11 18. Palmqvist, S. *et al.* Discriminative accuracy of plasma phospho-tau217 for
- 12 Alzheimer disease vs other neurodegenerative disorders. *JAMA* **324**, 772–781
- 13 (2020).
- 14 19. Janelidze, S. *et al.* Associations of Plasma Phospho-Tau217 Levels With Tau
- 15 Positron Emission Tomography in Early Alzheimer Disease. *JAMA Neurol.* **78**,
- 16 149–156 (2021).
- 17 20. Fitzpatrick, A. W. P. *et al.* Cryo-EM structures of tau filaments from Alzheimer's
- 18 disease. *Nature* **547**, 185–190 (2017).
- 19 21. Koss, D. J. *et al.* Soluble pre-fibrillar tau and β -amyloid species emerge in early
- 20 human Alzheimer's disease and track disease progression and cognitive decline.
- 21 *Acta Neuropathol.* **132**, 875–895 (2016).
- 22 22. Han, P. *et al.* A Quantitative Analysis of Brain Soluble Tau and the Tau Secretion
- 23 Factor. *J. Neuropathol. Exp. Neurol.* **76**, 44–51 (2017).
- 24 23. Sato, C. *et al.* Tau Kinetics in Neurons and the Human Central Nervous System.
- 25 *Neuron* **98**, 861–864 (2018).
- 26 24. Thijssen, E. H. *et al.* Diagnostic value of plasma phosphorylated tau181 in
- 27 Alzheimer's disease and frontotemporal lobar degeneration. *Nat. Med.* **26**, 387–397
- 28 (2020).
- 29 25. Lantero Rodriguez, J. *et al.* Plasma p-tau181 accurately predicts Alzheimer's
- 30 disease pathology at least 8 years prior to post-mortem and improves the clinical
- 31 characterisation of cognitive decline. *Acta Neuropathol.* **140**, 267–278 (2020).
- 32 26. Karikari, T. K. *et al.* Diagnostic performance and prediction of clinical progression
- 33 of plasma phospho-tau181 in the Alzheimer's Disease Neuroimaging Initiative. *Mol.*
- 34 *Psychiatry* **26**, 429–442 (2021).
- 35 27. Palmqvist, S. *et al.* Prediction of future Alzheimer's disease dementia using plasma
- 36 phospho-tau combined with other accessible measures. *Nat. Med.* **27**, 1034–1042

- 1 (2021).
- 2 28. Groot, C. *et al.* Phospho-tau with subthreshold tau-PET predicts increased tau
3 accumulation rates in amyloid-positive individuals. *Brain* (2022)
4 doi:10.1093/brain/awac329.
- 5 29. Mattsson-Carlgen, N. *et al.* Soluble P-tau217 reflects amyloid and tau pathology
6 and mediates the association of amyloid with tau. *EMBO Mol. Med.* **13**, e14022
7 (2021).
- 8 30. Therriault, J. *et al.* Association of Phosphorylated Tau Biomarkers With Amyloid
9 Positron Emission Tomography vs Tau Positron Emission Tomography. *JAMA*
10 *Neurol.* (2022) doi:10.1001/jamaneurol.2022.4485.
- 11 31. Smirnov, D. S. *et al.* Plasma biomarkers for Alzheimer’s Disease in relation to
12 neuropathology and cognitive change. *Acta Neuropathol.* **143**, 487–503 (2022).
- 13 32. Salvadó, G. *et al.* Specific associations between plasma biomarkers and
14 postmortem amyloid plaque and tau tangle loads. *EMBO Mol. Med.* e2463 (2023).
- 15 33. Guillozet-Bongaarts, A. L. *et al.* Tau truncation during neurofibrillary tangle
16 evolution in Alzheimer’s disease. *Neurobiol. Aging* **26**, 1015–1022 (2005).
- 17 34. Tagai, K. *et al.* High-Contrast In Vivo Imaging of Tau Pathologies in Alzheimer’s
18 and Non-Alzheimer’s Disease Tauopathies. *Neuron* **109**, 42–58.e8 (2021).
- 19 35. Endo, H. *et al.* A Machine Learning-Based Approach to Discrimination of
20 Tauopathies Using [18 F]PM-PBB3 PET Images. *Mov. Disord.* **37**, 2236–2246
21 (2022).
- 22 36. Schöll, M. *et al.* PET Imaging of Tau Deposition in the Aging Human Brain.
23 *Neuron* **89**, 971–982 (2016).
- 24 37. Ossenkoppele, R. *et al.* Discriminative Accuracy of [18F]flortaucipir Positron
25 Emission Tomography for Alzheimer Disease vs Other Neurodegenerative
26 Disorders. *JAMA* **320**, 1151–1162 (2018).
- 27 38. Dickerson, B. C. *et al.* The Cortical Signature of Alzheimer’s Disease: Regionally
28 Specific Cortical Thinning Relates to Symptom Severity in Very Mild to Mild AD
29 Dementia and is Detectable in Asymptomatic Amyloid-Positive Individuals. *Cereb.*
30 *Cortex* **19**, 497–510 (2008).
- 31 39. Venkatramani, A. & Panda, D. Regulation of neuronal microtubule dynamics by
32 tau: Implications for tauopathies. *Int. J. Biol. Macromol.* **133**, 473–483 (2019).
- 33 40. Zhang, F. *et al.* β -amyloid redirects norepinephrine signaling to activate the
34 pathogenic GSK3 β /tau cascade. *Sci. Transl. Med.* **12**, (2020).
- 35 41. He, Z. *et al.* Amyloid- β plaques enhance Alzheimer’s brain tau-seeded pathologies
36 by facilitating neuritic plaque tau aggregation. *Nat. Med.* **24**, 29–38 (2018).

- 1 42. Maia, L. F. *et al.* Changes in amyloid- β and Tau in the cerebrospinal fluid of
2 transgenic mice overexpressing amyloid precursor protein. *Sci. Transl. Med.* **5**,
3 194re2 (2013).
- 4 43. Karikari, T. K. *et al.* Diagnostic performance and prediction of clinical progression
5 of plasma phospho-tau181 in the Alzheimer's Disease Neuroimaging Initiative.
6 *bioRxiv* (2020) doi:10.1101/2020.07.15.20154237.
- 7 44. Thijssen, E. H. *et al.* Plasma phosphorylated tau 217 and phosphorylated tau 181 as
8 biomarkers in Alzheimer's disease and frontotemporal lobar degeneration: a
9 retrospective diagnostic performance study. *Lancet Neurol.* **20**, 739–752 (2021).
- 10 45. Benussi, A. *et al.* Classification accuracy of blood-based and neurophysiological
11 markers in the differential diagnosis of Alzheimer's disease and frontotemporal
12 lobar degeneration. *Alzheimers. Res. Ther.* **14**, 155 (2022).
- 13 46. Mielke, M. M. *et al.* Comparison of Plasma Phosphorylated Tau Species With
14 Amyloid and Tau Positron Emission Tomography, Neurodegeneration, Vascular
15 Pathology, and Cognitive Outcomes. *JAMA Neurol.* **78**, 1108–1117 (2021).
- 16 47. Janelidze, S. *et al.* Head-to-head comparison of 10 plasma phospho-tau assays in
17 prodromal Alzheimer's disease. *Brain* (2022) doi:10.1093/brain/awac333.
- 18 48. Milà-Alomà, M. *et al.* Plasma p-tau231 and p-tau217 as state markers of amyloid- β
19 pathology in preclinical Alzheimer's disease. *Nat. Med.* **28**, 1797–1801 (2022).
- 20 49. Suárez-Calvet, M. *et al.* Novel tau biomarkers phosphorylated at T181, T217 or
21 T231 rise in the initial stages of the preclinical Alzheimer's continuum when only
22 subtle changes in A β pathology are detected. *EMBO Mol. Med.* **12**, e12921 (2020).
- 23 50. Dujardin, S. *et al.* Tau molecular diversity contributes to clinical heterogeneity in
24 Alzheimer's disease. *Nat. Med.* **26**, 1256–1263 (2020).
- 25 51. García-Sierra, F., Ghoshal, N., Quinn, B., Berry, R. W. & Binder, L. I.
26 Conformational changes and truncation of tau protein during tangle evolution in
27 Alzheimer's disease. *J. Alzheimers. Dis.* **5**, 65–77 (2003).
- 28 52. Bondareff, W. *et al.* Molecular analysis of neurofibrillary degeneration in
29 Alzheimer's disease. An immunohistochemical study. *Am. J. Pathol.* **137**, 711–723
30 (1990).
- 31 53. Horowitz, P. M. *et al.* Early N-terminal changes and caspase-6 cleavage of tau in
32 Alzheimer's disease. *J. Neurosci.* **24**, 7895–7902 (2004).
- 33 54. Bloom, G. S. Amyloid- β and tau: the trigger and bullet in Alzheimer disease
34 pathogenesis. *JAMA Neurol.* **71**, 505–508 (2014).
- 35 55. Cai, Y. *et al.* Initial levels of β -amyloid and tau deposition have distinct effects on
36 longitudinal tau accumulation in Alzheimer's disease. *Alzheimers. Res. Ther.* **15**, 30

- 1 (2023).
- 2 56. Barthélemy, N. R. *et al.* A soluble phosphorylated tau signature links tau, amyloid
3 and the evolution of stages of dominantly inherited Alzheimer's disease. *Nat. Med.*
4 **26**, 398–407 (2020).
- 5 57. Kametani, F. *et al.* Comparison of Common and Disease-Specific Post-translational
6 Modifications of Pathological Tau Associated With a Wide Range of Tauopathies.
7 *Front. Neurosci.* **14**, 581936 (2020).
- 8 58. Sato, C. *et al.* MAPT R406W increases tau T217 phosphorylation in absence of
9 amyloid pathology. *Ann Clin Transl Neurol* **8**, 1817–1830 (2021).
- 10 59. Kurihara, M. *et al.* CSF P-Tau181 and Other Biomarkers in Patients With Neuronal
11 Intracellular Inclusion Disease. *Neurology* **100**, e1009–e1019 (2023).
- 12 60. Barthélemy, N. R. *et al.* Cerebrospinal fluid phospho-tau T217 outperforms T181 as
13 a biomarker for the differential diagnosis of Alzheimer's disease and PET
14 amyloid-positive patient identification. *Alzheimers. Res. Ther.* **12**, 26 (2020).
- 15 61. Blennow, K. *et al.* Cerebrospinal fluid tau fragment correlates with tau PET: a
16 candidate biomarker for tangle pathology. *Brain* **143**, 650–660 (2020).
- 17 62. Horie, K. *et al.* CSF MTBR-tau243 is a specific biomarker of tau tangle pathology
18 in Alzheimer's disease. *Nat. Med.* **29**, 1954–1963 (2023).
- 19 63. Tagai, K. *et al.* An optimized reference tissue method for quantification of tau
20 protein depositions in diverse neurodegenerative disorders by PET with
21 18F-PM-PBB3 (18F-APN-1607). *Neuroimage* **264**, 119763 (2022).
- 22 64. Klunk, W. E. *et al.* The Centiloid Project: Standardizing quantitative amyloid
23 plaque estimation by PET. *Alzheimers. Dement.* **11**, 1 (2015).

24 **Funding**

25 This study was supported in part by AMED under Grant Numbers JP18dm0207018,
26 JP19dm0207072, JP18dk0207026, JP19dk0207049, 21wm0425015h0001, and
27 20356533; MEXT KAKENHI under Grant Numbers JP16H05324 and JP18K07543;
28 JST under Grant Numbers JPMJCR1652 and JPMJMS2024; and the Kao Research
29 Council for the Study of Healthcare Science, Biogen Idec Inc. and APRINOIA
30 Therapeutics.

31 **Acknowledgements**

32 The authors thank all patients and their caregivers for participation in this study, as
33 well as clinical research coordinators, PET and MRI operators, radiochemists, and
34 research ethics advisers at QST for their assistance with the current projects. We thank
35

APRINOIA Therapeutics for kindly sharing a precursor of ^{18}F -florzorotau. The authors acknowledge support with the recruitment of patients by Shunichiro Shinagawa at the Department of Psychiatry, Jikei University School of Medicine; Shigeki Hirano at the Department of Neurology, Chiba University; Taku Hatano, Yumiko Motoi, and Shinji Saiki at the Department of Neurology, Juntendo University School of Medicine; Ikuko Aiba at the Department of Neurology, National Hospital Organization Higashinagoya National Hospital; Yasushi Shiio and Tomonari Seki at the Department of Neurology, Tokyo Teishin Hospital; Hisaomi Suzuki at the National Hospital Organization Shimofusa Psychiatric Medical Center.

Author contributions

Kenji Tagai, Harutsugu Tatebe: Conceptualization, Methodology, Formal analysis, Writing - original draft. **Sayo Matsuura, Zhang Hong:** Measurement of samples. **Naomi Kokubo, Kiwamu Matsuoka, Hironobu Endo, Asaka Oyama, Kosei Hirata, Hitoshi Shinotoh, Yuko Kataoka, Hideki Matsumoto, Masaki Oya, Shin Kurose, Keisuke Takahata, Masanori Ichihashi, Manabu Kubota, Chie Seki, Hitoshi Shimada, Yuhei Takado:** Collection of clinical data. **Kazunori Kawamura, Ming-Rong Zhang:** Radioligand synthesis. **Yoshiyuki Soeda, Akihiko Takashima:** Assay validation. **Makoto Higuchi, Takahiko Tokuda:** Conceptualization, Writing - review & editing, Funding acquisition, Supervision

Competing interests

Hitoshi Shimada, Ming-Rong Zhang, and Makoto Higuchi hold patents on compounds related to the present report (JP 5422782/EP 12 884 742.3/CA2894994/HK1208672).

Table 1. Demographic and blood biomarker data of the participants.

	CN	AD	PSP	FTLD
Demographics				
Number	40	48	50	26
Age	66.0 (10.4)	69.3 (11.4)	71.2 (7.5)	65.0 (11.4)
Gender (male/female)	21/19	27/21	21/29	18/8
Years of schooling	14.8 (1.6)	13.9 (2.2)	13.6 (2.6)	14.0 (2.8)
MMSE	29.3 (1.0) [†]	21.9 (4.1) [*]	24.8 (5.8) ^{*†}	23.8 (6.1) [*]
FAB	16.7 (1.2) [†]	13.0 (3.0) [*]	12.0 (3.6) [*]	11.0 (4.8) [*]
CDR (0.5/1/2/3)	N/A	23/20/4/1	N/A	N/A
PSPRS	N/A	N/A	38.1 (18.2)	N/A
Blood biomarkers				
Aβ42/40	0.093 (0.020) [†]	0.067 (0.020) [†]	0.096 (0.048) [†]	0.089 (0.022) [†]
N-p-tau181 (pg/mL)	1.82 (0.79) [†]	4.07 (1.52) [*]	2.27 (1.06) [†]	2.25 (1.25) [†]
mid-p-tau181 (pg/mL)	0.83 (0.65) [†]	2.30 (1.31) [*]	1.56 (0.91) [*]	0.96 (0.63) [†]
NfL (pg/mL)	19.5 (12.5) ^{†‡}	33.2 (21.3) ^{*‡}	58.3 (39.7) ^{*†}	51.8 (39.3) [*]

CN, cognitively normal; AD, Alzheimer's disease; PSP, progressive supranuclear palsy; FTLD, frontotemporal degeneration; MMSE, Mini-Mental State Examination; FAB, Frontal Assessment Battery; CDR, Clinical Dementia Rating scale; PSPRS, progressive supranuclear palsy rating scale; N/A, not applicable; Aβ, amyloid beta; N-p-tau181, phosphorylated tau181 measured using the commercial kit directed to the C-terminally truncated N-terminal fragment of p-tau (Simoa pTau-181 V2.1 Assay, Quanterix); mid-p-tau181, phosphorylated tau181 measured using the originally developed immunoassay directed to both the N- and C-terminally truncated p-tau181 fragments; NfL, neurofilament light chain.

Values are presented as mean ± standard deviation.

^{*}, Significant difference between CN, [†], between AD, [‡], between PSP, $P < 0.05$ (corrected by Dunn's multiple comparisons)

Table 2. Performance of mid-p-tau181 in discriminating tau PET status determined using three different methods of evaluating brain tau burden on tau PET in the cognitively normal and AD continuum subjects

	Sensitivity (%)	Specificity (%)	Cutoff value (pg/mL)	AUC
Braak staging	62.8	92.5	1.76	0.859
Temporal meta SUVR	71.8	88.6	1.69	0.855
AD tau score	70.5	88.1	1.62	0.870

All parameters were estimated from receiver operating characteristic curve analyses. We set each cutoff value according to Youden index obtained in the respective receiver operating characteristic analyses. SUVR, standardized uptake value ratio; AUC, area under the receiver operating characteristic curve.

Figure legends

Figure 1. Correlations between plasma mid-p-tau levels and tau PET results in the subjects with AD continuum.

(A) The correlation between plasma mid-p-tau181 levels and ^{18}F -florzorotau tau PET is depicted through its topographical representation ($p < 0.05$, family-wise error corrected).

(B, C) The correlation between plasma mid-p-tau181 levels and tau PET tracer accumulation in each ROI is portrayed via scatter plots. Pearson's correlation analysis was employed to calculate the r and p values. Statistical significance was established at $p < 0.0125$, corrected for multiple comparisons using the Bonferroni method based on the number of ROIs. Regression analysis, indicated by a straight or curved line, depicts the preferred model, with its goodness of fit quantified using the R^2 value.

SUVR, standardized uptake value ratio; AD tau score, a machine learning-based measure indicating AD-related features in tau PET images.

Mid-p-tau181, phosphorylated tau181 measured using the originally developed immunoassay directed to both N- and C-terminally truncated p-tau181 fragments.

Figure 2 Correlation between plasma N-p-tau levels measured using a conventional p-tau assay and tau PET results in the subjects with AD continuum.

(A) The correlation between plasma N-p-tau181 levels and tau PET results is demonstrated through its topographical representation ($p < 0.05$, uncorrected).

(B, C) The correlation between plasma N-p-tau181 levels and tau PET tracer accumulation in each ROI is depicted via scatter plots. Pearson's correlation analysis was utilized to calculate the r and p values. The preferred model, indicated by regression analysis, is depicted by a straight or curved line, with its goodness of fit quantified using the R^2 value.

SUVR, standardized uptake value ratio; AD tau score, a machine learning-based measure indicating AD-related features in tau PET images.

N-p-tau181, phosphorylated tau181 measured using the Simoa pTau-181 V2.1 Assay kit (Quanterix).

Figure 3. Scatter plots and ROC curves of the mid-p-tau181 showing its ability to discriminate between tau PET statuses determined by three different approaches in the cognitively normal and AD continuum subjects.

Scatterplots (A) and ROC curves (B) illustrating the relationship between mid-p-tau181 levels and positive/negative tau PET results as determined by three different methods. In the scatterplot, CN subjects are represented in purple, whereas AD continuum patients are depicted in blue. The dotted line represents the mid-p-tau181 cutoff calculated based on each approach. $p < 0.0001$ (****), as assessed by Mann–Whitney U test.

Figure 4. Correlations between plasma mid-p-tau and N-p-tau levels and MRI structural images in the subjects with AD continuum.

(A) The correlation between p-tau181 measured using the mid-p-tau181 or N-p-tau assay and brain atrophy is depicted through its topographical representation ($p < 0.05$, uncorrected).

(B) The correlation between plasma mid-p-tau181 and N-p-tau levels measured using each assay and the thinning of the AD cortical signature is demonstrated via scatter plots. Pearson's correlation analysis was utilized to calculate.

N-p-tau181, phosphorylated tau181 measured using the Simoa pTau-181 V2.1 Assay kit (Quanterix); mid-p-tau181, phosphorylated tau181 measured using the originally developed immunoassay directed to both N- and C-terminally truncated p-tau181 fragments.

Figure 5. Comparative analyses of blood biomarkers across the clinical diagnosis groups and between the amyloid PET status.

(A) The data distribution is portrayed using scatter plots, with group differences having been evaluated through the Kruskal–Wallis test. Statistically significant differences are denoted as follows: $p < 0.0001$ (****), $p = 0.0004$, or 0.0010 (***), $p = 0.0070$ (**), and non-significant at $p < 0.05$ (ns), as determined using Dunn's multiple comparisons.

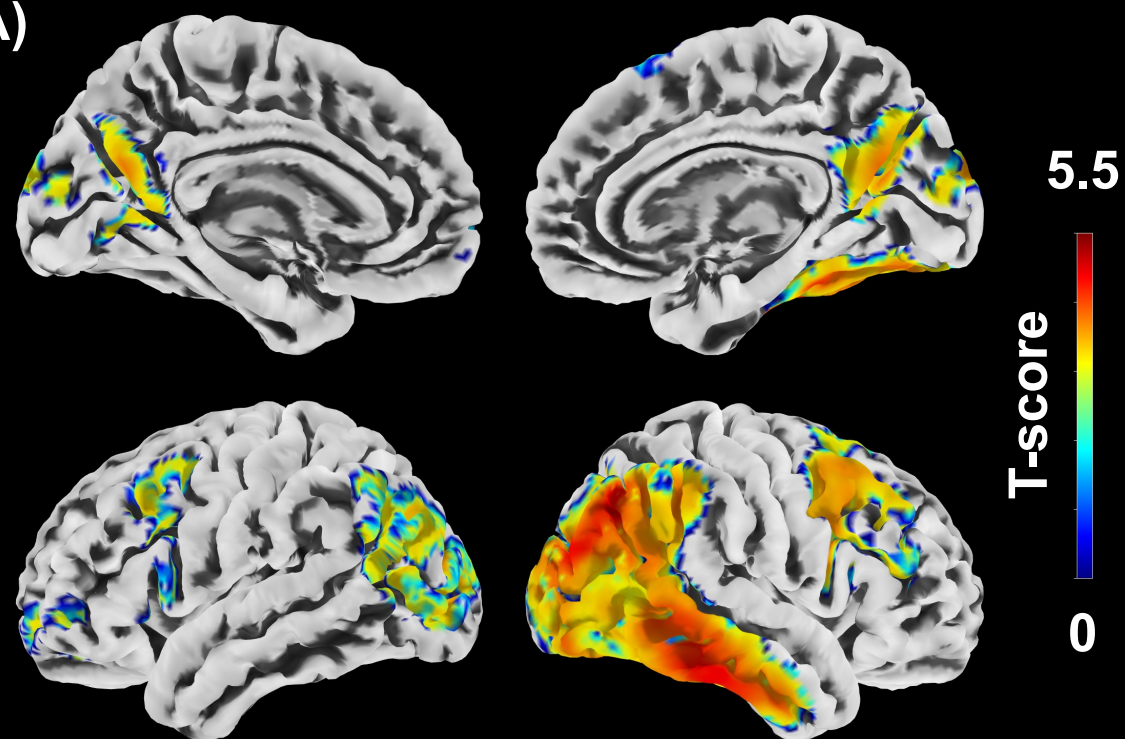
(B) ROC curves were utilized to differentiate AD from other groups determined according to qualitative findings of amyloid PET. The corresponding AUC values are listed.

CN, cognitively normal; AD, Alzheimer's disease; PSP, progressive supranuclear palsy; FTL, frontotemporal degeneration; A β , amyloid beta; N-p-tau181, phosphorylated tau181 measured with the Simoa pTau-181 V2.1 Assay kit (Quanterix); mid-p-tau181, phosphorylated tau181 measured using the originally developed immunoassay directed to both N- and C-terminally truncated p-tau181 fragments; NfL, neurofilament light chain; ROC, Receiver Operating Characteristic; AUC, area under the ROC curve.

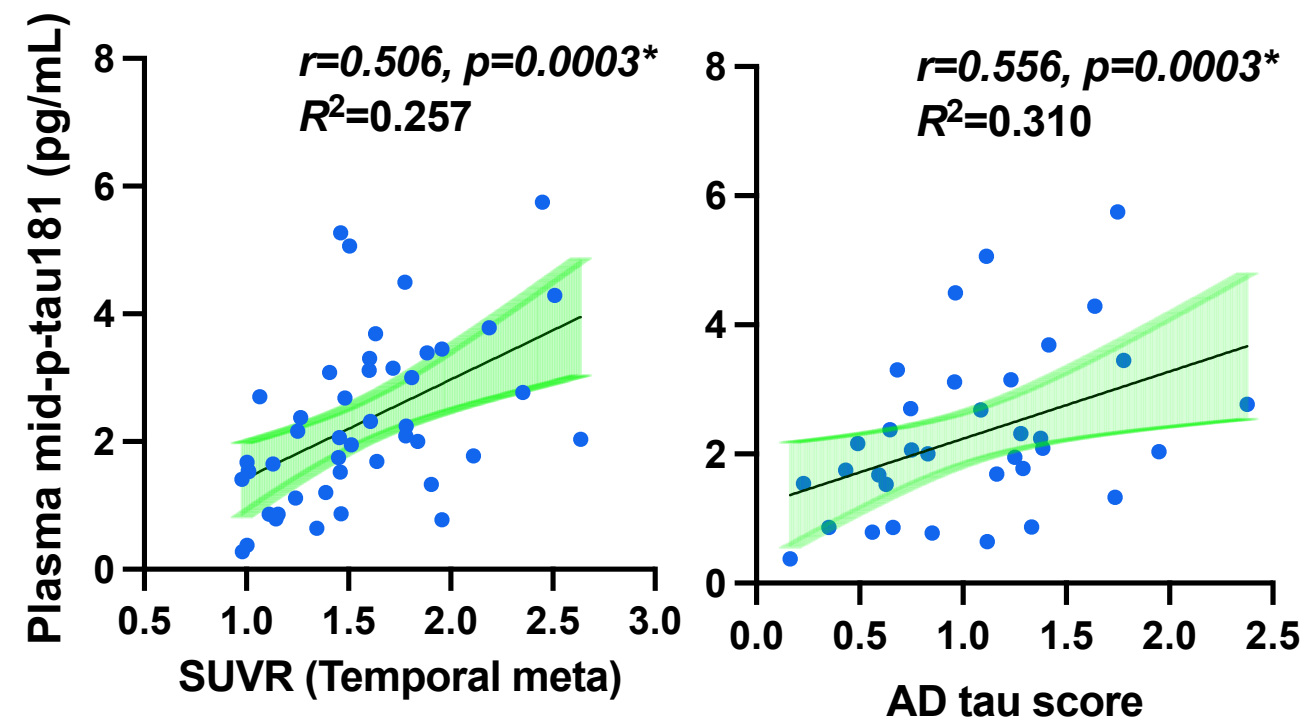
1 **Figure 6. Trajectories of the imaging and plasma A/T/N biomarkers along with the**
2 **decline in the MMSE scores.**
3 Trajectories of the changes in imaging (A) and blood-based (B) A/T/N biomarkers with
4 the decline in MMSE scores. The relationship between MMSE scores of the CN and AD
5 continuum subjects and the z-scores of each biomarker is presented as a regression line
6 that is either straight or sigmoidal, with the best fitting model being selected. The
7 biomarkers were distinguished using red, green, and blue for both imaging and
8 blood-based biomarkers, whereas N-p-tau181 was presented separately in purple. The
9 dotted line indicates z-score = 1.
10

Tau PET vs Plasma Mid-p-tau181

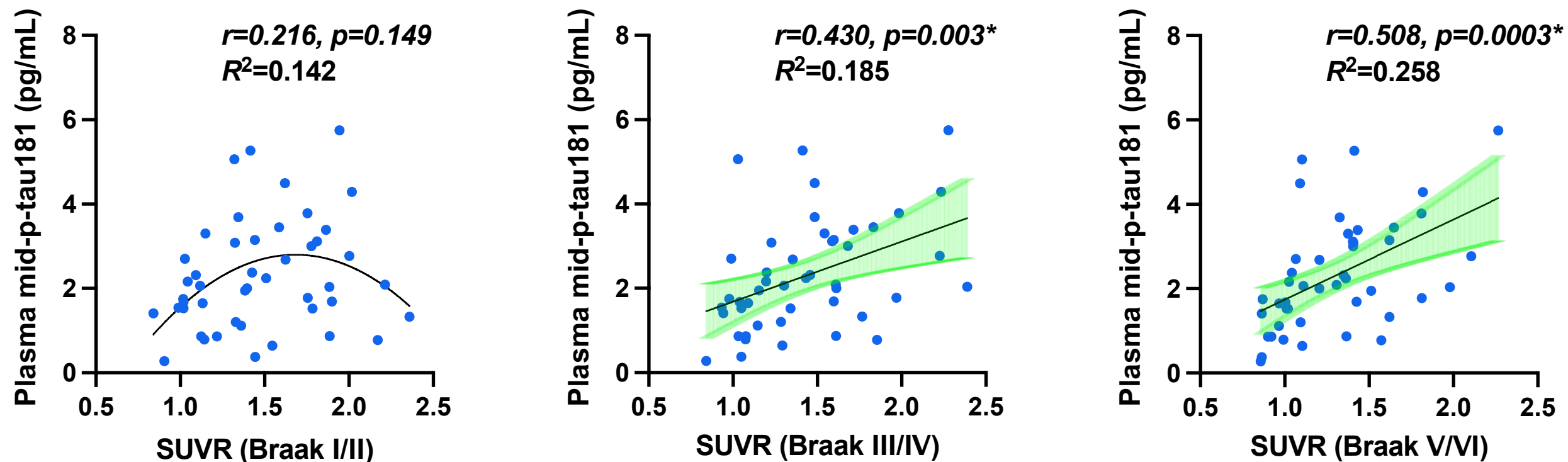
(A)



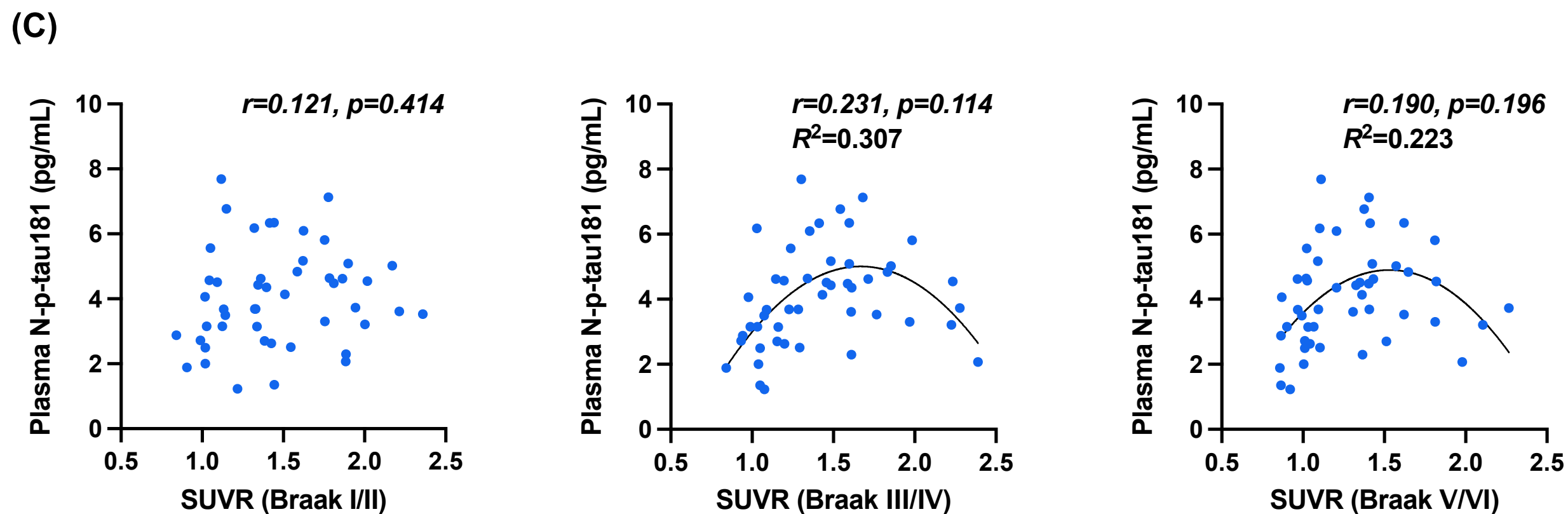
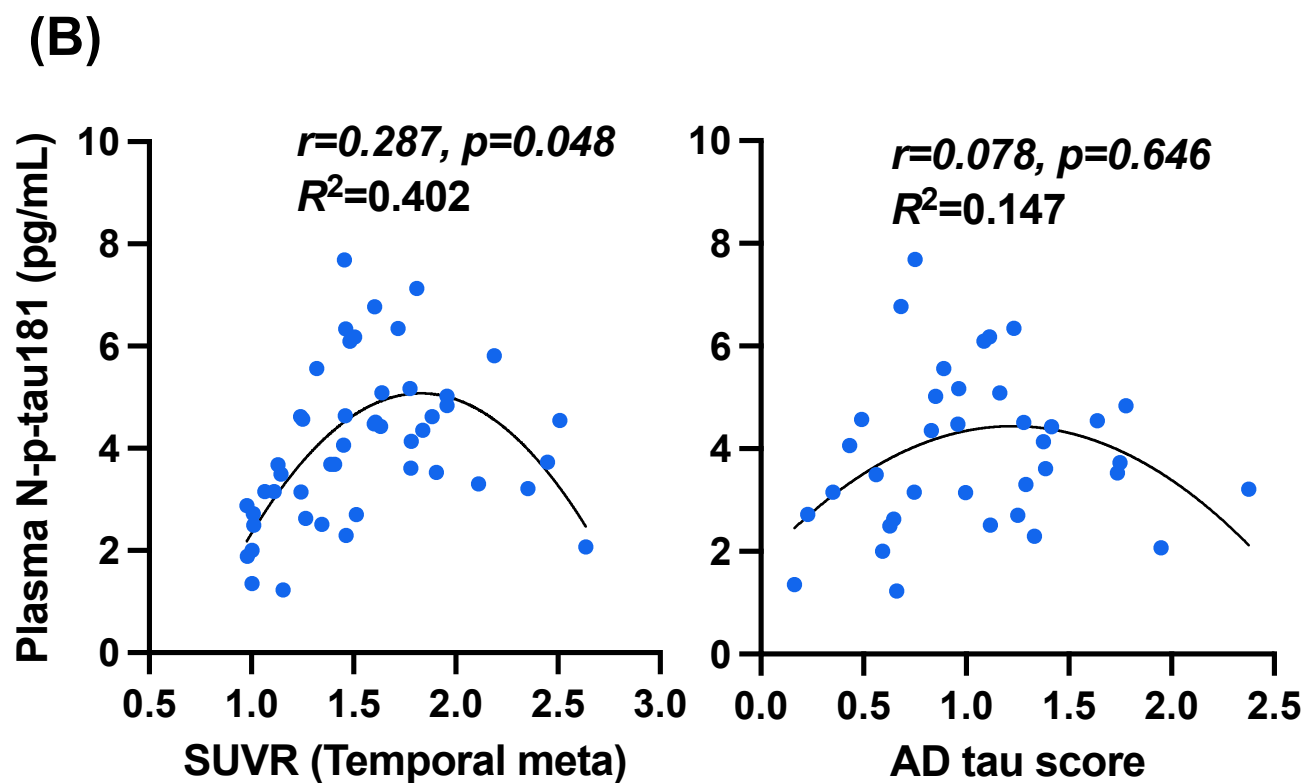
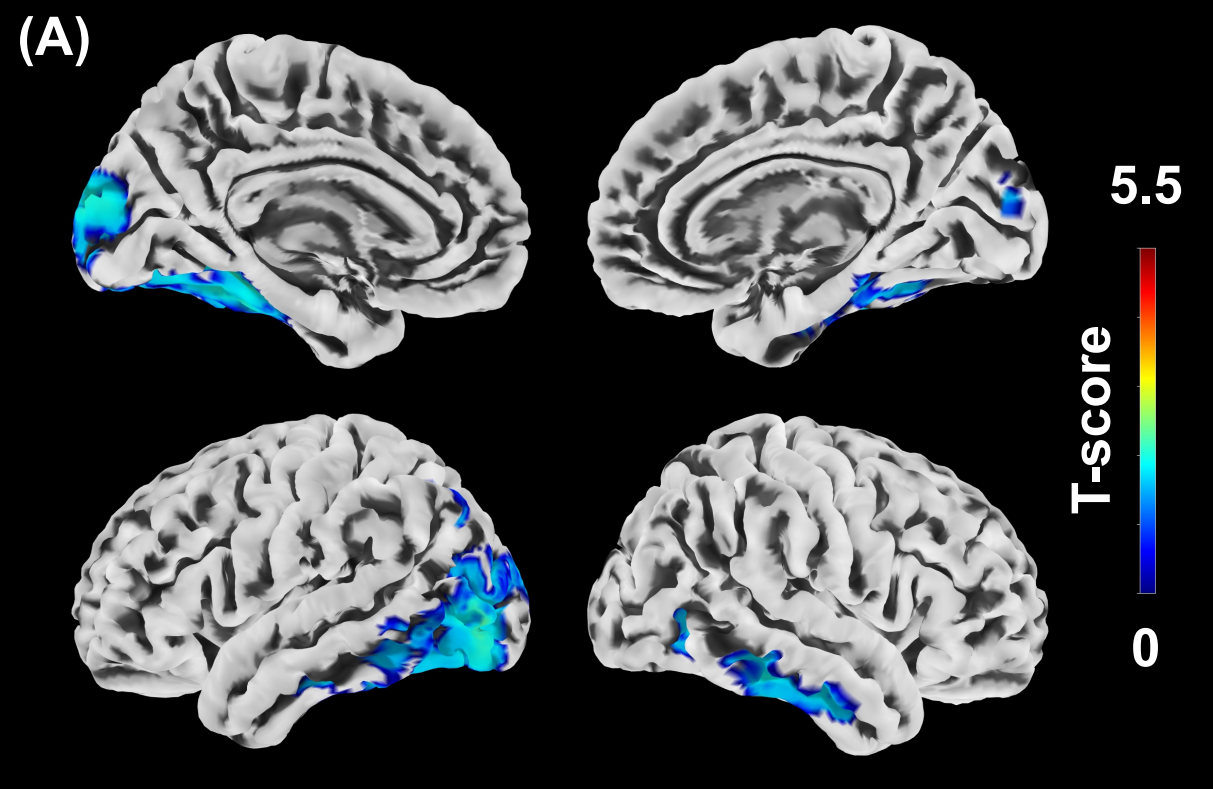
(B)



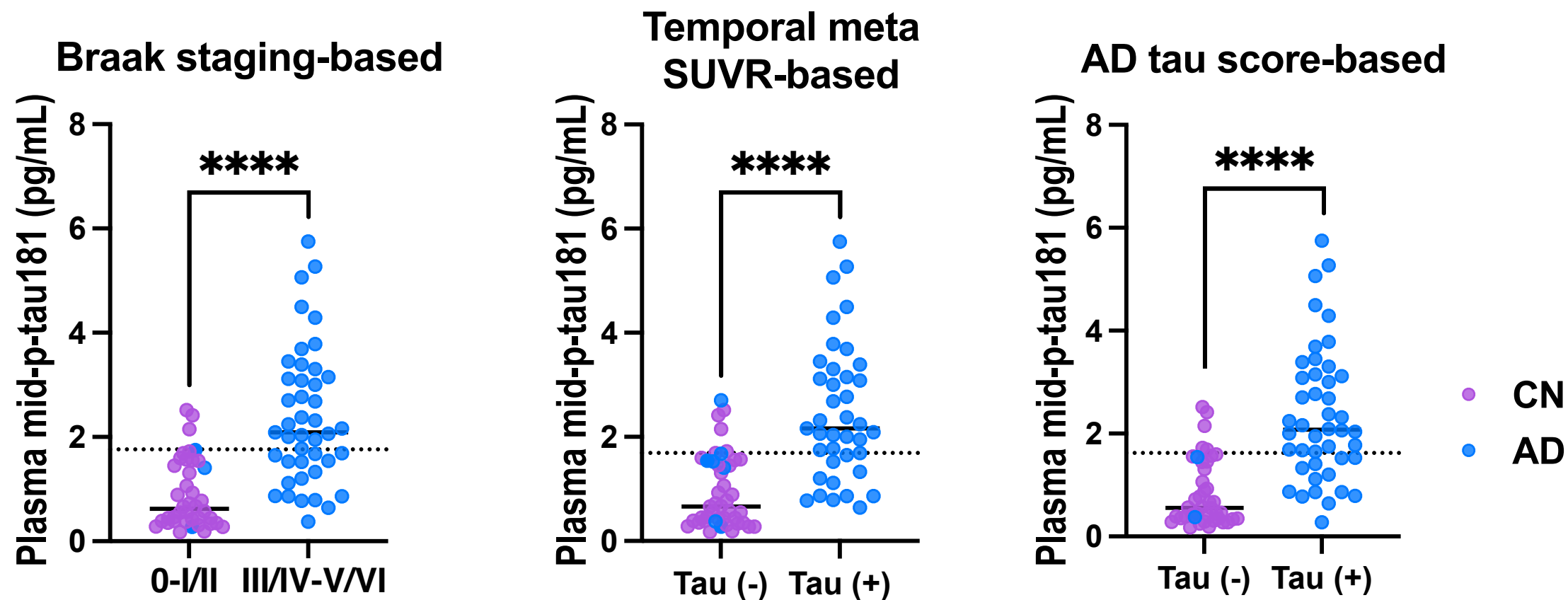
(C)



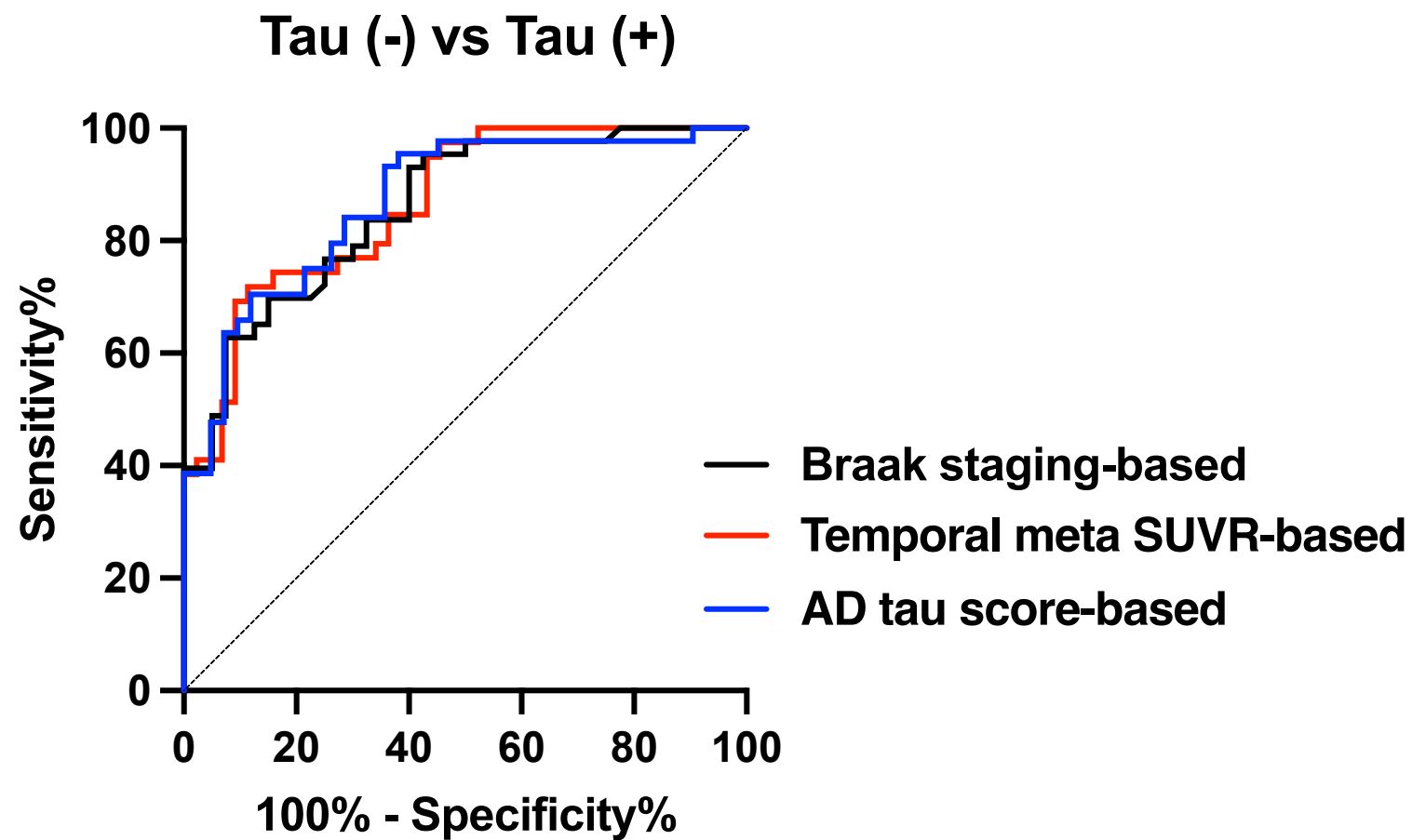
Tau PET vs Plasma N-p-tau181



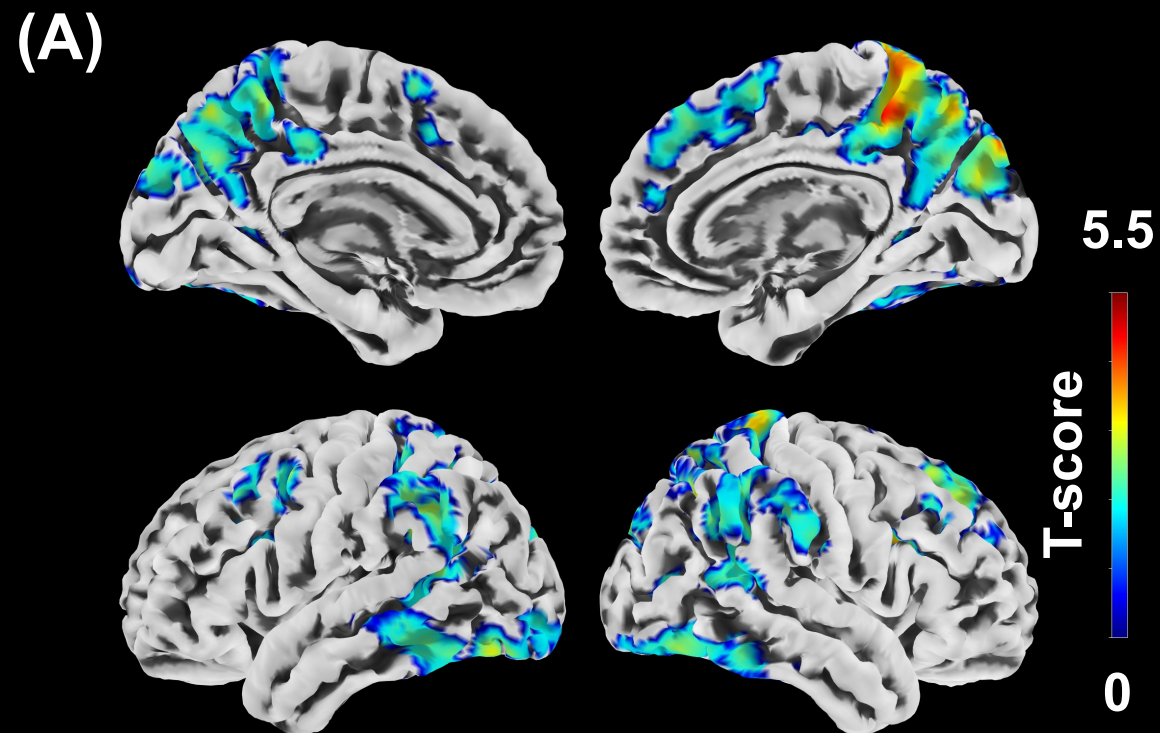
(A)



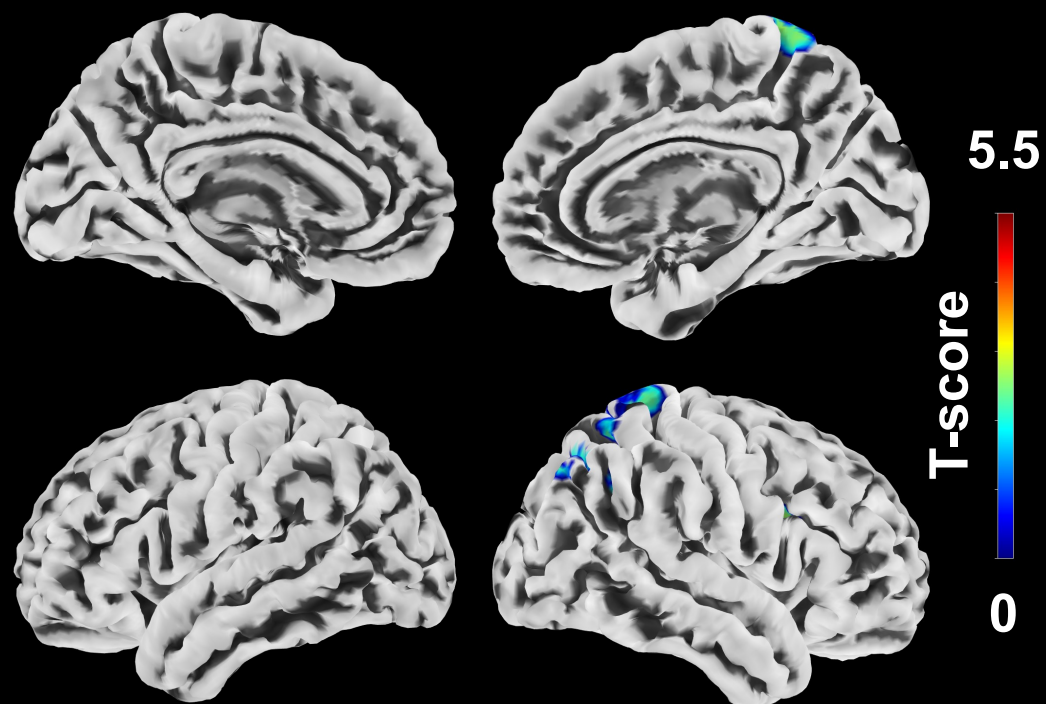
(B)



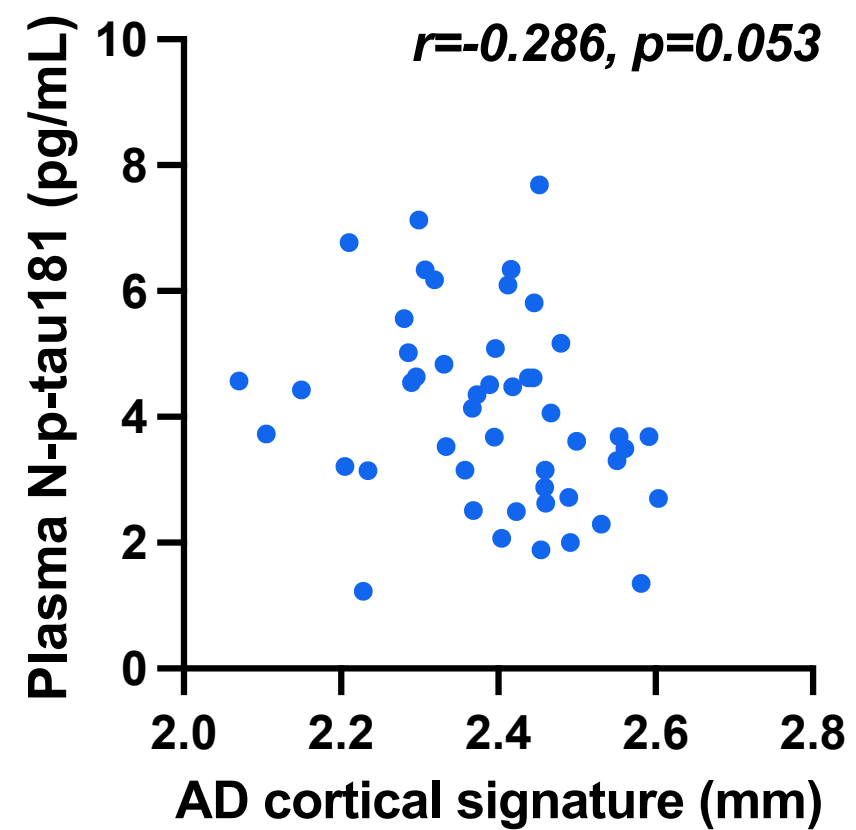
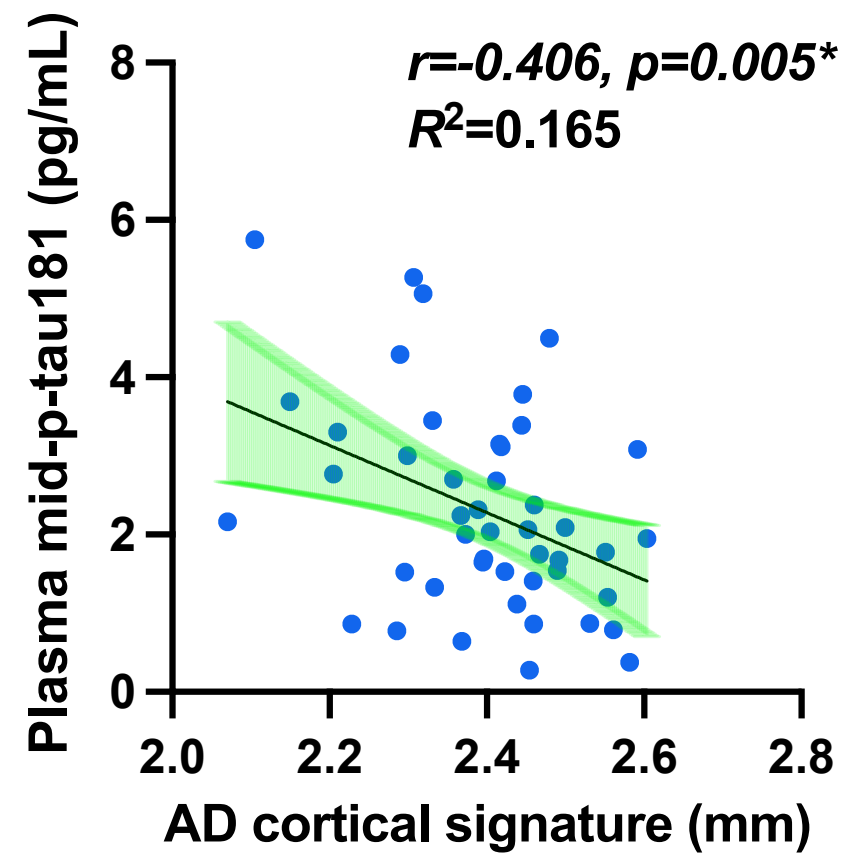
MRI vs Plasma Mid-p-tau181



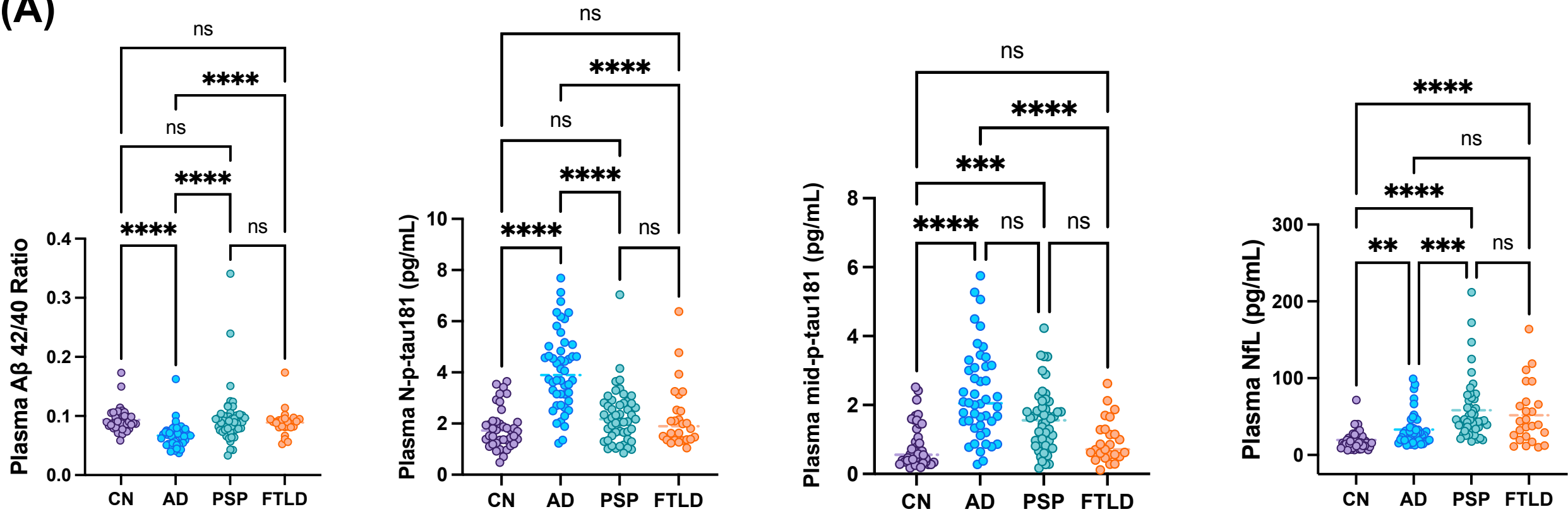
MRI vs Plasma N-p-tau181



(B)

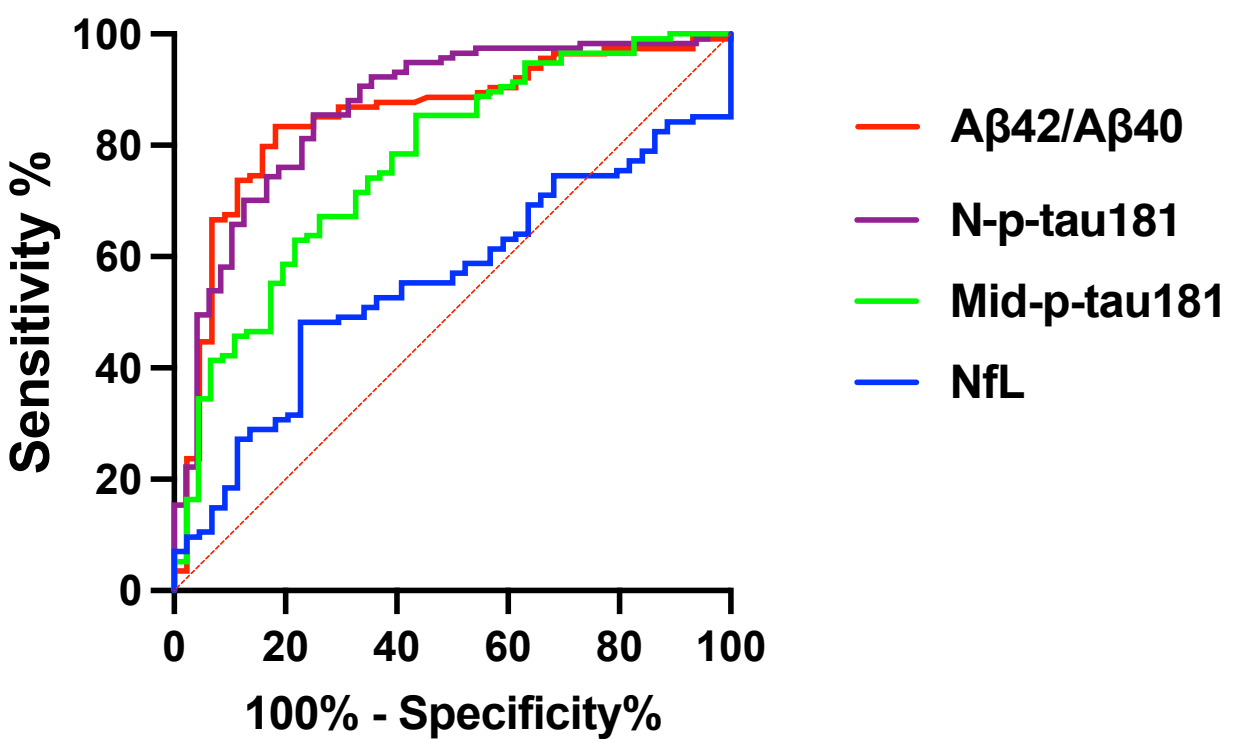


(A)



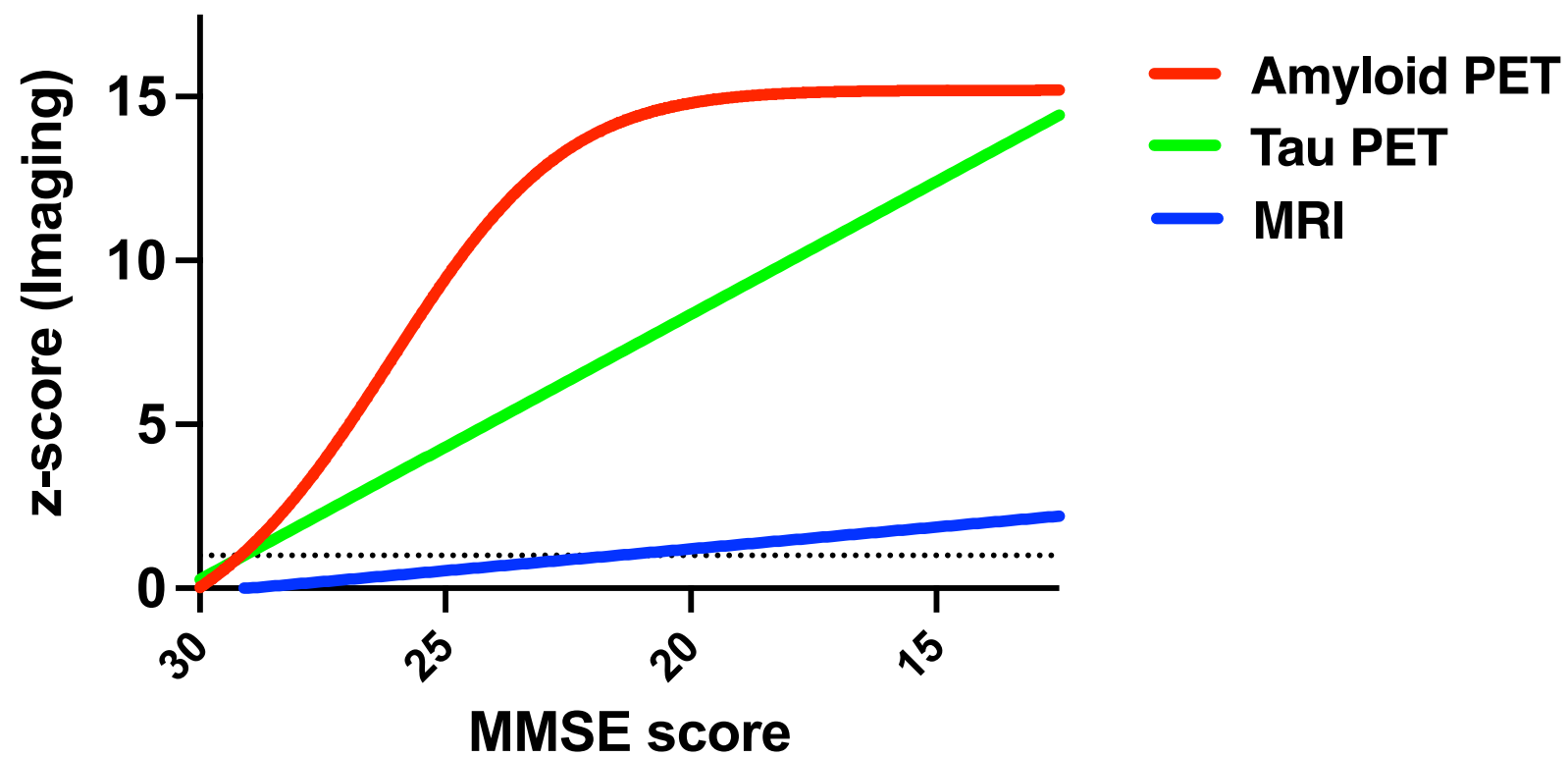
(B)

Amyloid (+) vs Amyloid (-)



	AUC values
Aβ42/40	0.714
N-p-tau181	0.905
Mid-p-tau181	0.844
NfL	0.641

(A)



(B)

